the ring shaped packings should be preferred over the spheres for cost-effective operation of the packed-bed air heaters.

REFERENCES

1. H. P. Garg, B. Bandyopadhyay and V. K. Sharma, *Energy Convers. Mgmt* **21**, 275 (1981).
2. Y. Demirel and S. Kunc, *Energy Convers. Mgmt* **27**, 317 (1987).
3. V. K. Sharma, H. P. Garg, S. Sharma and R. A. Roy, *Int. J. Energy Syst.* **8**, 106 (1988).
4. C. Choudhury and H. P. Garg, A study on the performance of the air heating collectors with packed air flow passage. *Sol. Energy*. In press (1992).

APPENDIX 1

$$U_t = h_{w1a} + h_{r1a}$$
$$h_{w1a} = 5.7 + 3.8 \times 1.5$$
$$h_{r1a} = \epsilon_{1\sigma}(T_1^2 + T_s^2)(T_1^2 - T_s^2)/(T_1 - T_a)$$
$$T_s = (0.0552)\,(T_a)^{1.5}$$
$$h_{r12} = \frac{(T_1^2 + T_2^2)(T_1 + T_2)}{\frac{1}{\epsilon_1} + \frac{1}{\epsilon_2} - 1}$$
$$h_{c1f} = h_{c2f} = \mathrm{Nu}_H k_f / D_H \text{ (for Type I)}$$
$$\mathrm{Nu}_H = 0.033\,\mathrm{Re}_H^{0.8}\,\mathrm{Pr}^{1/3}$$
$$\mathrm{Re}_H = G D_H / \mu$$
$$\mathrm{Pr} = \mu C_f / k_f$$
$$h_{c1f} = h_{c2f} = \mathrm{Nu}_p k_f / D_p \text{ (for Types II and III)}$$
$$\mathrm{Nu}_p = 0.2\,\mathrm{Re}_p^{0.8}\,\mathrm{Pr}^{1/3}$$
$$\mathrm{Re}_p = G D_p / \mu$$
$$h_{cpf} = \left(\frac{1}{h_{pf}} + \frac{D_p}{Bk_p}\right)^{-1}$$
$$h_{pf} = \mathrm{Nu}_{pf} k_f / D_p$$
$$\mathrm{Nu}_{pf} = \frac{0.255}{\epsilon'}\,\mathrm{Re}_p^{2/3}\,\mathrm{Pr}^{1/3}$$
$$h_{rp1} = \frac{\sigma(T_1^2 + T_p^2)(T_1 + T_p)}{\frac{1}{\epsilon_1} + \frac{1}{\epsilon_p} - 1}$$
$$h_{rp2} = \frac{\sigma(T_2^2 + T_p^2)(T_2 + T_p)}{\frac{1}{\epsilon_2} + \frac{1}{\epsilon_p} - 1}$$
$$U_b = k_i / t$$

APPENDIX 2

$$P = \dot{m}_f \Delta P / \rho_f$$
$$\Delta P = 2f \frac{G^2}{\rho_f} \frac{L}{D_H} \text{ (for Type I)}$$
$$f = 0.059\,\mathrm{Re}_H^{-0.2}$$
$$\Delta P = f \frac{G^2}{\rho_f} \frac{L}{D_p} \frac{(1 - \epsilon')}{\epsilon'^3} \text{ (for Types II and III)}$$
$$f = 150\left[\frac{(1 - \epsilon')}{\mathrm{Re}_p} + 1.75\right].$$

AIVC 11155

Energy Convers. Mgmt Vol. 34, No. 2, pp. 139–146, 1993
Printed in Great Britain.

0196-8904/93 $5.00 + 0.00

CALCULATIONS AND STATISTICAL ANALYSIS OF THE ENVIRONMENTAL COOLING POWER INDEX FOR ATHENS, GREECE

C. BALARAS,† I. TSELEPIDAKI, M. SANTAMOURIS and D. ASIMAKOPOULOS

Laboratory of Meteorology, Department of Physics, University of Athens, Ippokratous 33, GR106 80 Athens, Greece

(Received 22 July 1991; received for publication 17 April 1992)

Abstract—The dry cooling power index, representing summer comfort conditions, is calculated and statistically analysed for Athens, Greece using a 13-yr hourly database of meteorological parameters from measurements taken at the National Observatory of Athens. Information for energy analysts and climatologists, contributing towards more accurate analysis of the summer indoor and outdoor comfort conditions are also included.

Cooling power index Summer comfort Athens Greece

INTRODUCTION

Achievement of thermal comfort conditions during the summer period is of high priority especially for Southern European countries. Unpleasant climatic conditions and increased living standards have promoted the use of conventional as well as passive and hybrid cooling systems. It has been reported [1], that, due to the serious heat waves observed in Greece during the late 1980s, there has been an increase of about 800% in annual purchases of air-conditioning units. In the total world market, an increase of 300% in sales of conventional air-conditioning units has been registered for the period 1976–1985, presenting today a market turn in-excess-of 20 billion U.S. dollars [2]. On the other hand, a significant penetration of passive and hybrid cooling techniques in providing optimal interior conditions has been reported during the last few years [3].

Effective energy design of buildings as well as appropriate sizing of conventional, passive, and hybrid cooling systems requires knowledge of:

(a) The primary climatic data, and
(b) The distribution of discomfort conditions occurring at a given location.

While the required climatic data for Athens have been extensively analysed [4, 5], very little information is available on the distribution of comfort conditions for energy purposes in the area. In general, information on discomfort conditions is usually given for special events, like heat waves [6], which cannot be used for energy purposes.

Evaluation of discomfort conditions is mainly based on the calculation of human biometeorological indices which are based on various climatic parameters, like the dry bulb temperature, wind velocity, humidity, clothing, etc. A synoptic presentation of 30 biometeorological indices is given elsewhere [7].

The cooling power index proposed by Vinje [8], has gained an increasing acceptance in representing summer comfort conditions. In the following discussion, a statistical and persistence analysis of the cooling power index for Athens, Greece will be presented.

The present work primarily aims to provide necessary information to energy analysts and climatologists, contributing towards more accurate analysis of the summer indoor and outdoor comfort conditions.

†To whom all correspondence should be addressed at: Protechna Ltd, Society for Appropriate Technologies, Themistokleous 87, 10683 Athens, Greece.

THE COOLING POWER INDEX

The combination of meteorological parameters, as in the case of ambient temperature and wind, can cause different sensations of comfort to human beings. One way to quantify the effect of these environmental parameters on humans, is by a quantity termed the dry "cooling power" of the environment [8].

The cooling power represents the combined effects of ambient temperature and wind on the sensation of comfort they cause to humans. Numerous empirical correlations of these variables are available in the literature, which express the dry cooling power as a linear function of the body and the air temperature difference and a power of the wind speed. Most of the available correlations have been compared with observations and are included in Ref. [8]. The heat-loss correlation which is suggested by Vinje is selected for the present work and is given by,

$$H = 20.52\, V^{0.42}\,(36.5 - T) \quad (1)$$

where

H = cooling power (kcal/m^2 h)
V = wind speed (m/s)
T = dry bulb air temperature (°C).

In this case, the calculations of the dry cooling power were performed using hourly measurements of the dry bulb temperature and wind speed from the National Observatory of Athens, for a period of 13 yr (1977–1989), and for the cooling period of May–September.

The calculated H values are related to the corresponding sensation (hot, mild, cool, cold, etc.) experienced by humans based on a properly devised scale [8]. The sensation scale, for the dry cooling values, is shown in Table 1. These sensations are caused from a combination of low or high temperatures with the corresponding wind speed. Thus, the estimated sensations are representative of the prevailing climatological conditions and their effects on the thermal balance of humans with the environment.

STATISTICAL ANALYSIS

Daily distribution

The daily distribution of the various sensations for all 13 yr is shown in Fig. 1. Given for each hour is the percentage of the total number of occurrences for a particular sensation of that hour to the total number of possible occurrences.

The distribution of the hot hours is approximately constant throughout the 24-h. During the months of July and August, there is a maximum around the mid-afternoon hours and a minimum around the 20:00 LST. The lowest frequency number of hot hours is observed for the whole daily distribution in May, while the maximum is observed in July. June and September are lagging July, with August falling only a few percentages below July.

The hours which are labelled as mild, have an approximately constant behaviour throughout the 24-h monthly distributions, with the month of June exceeding all other monthly percentage distributions (see Fig. 2).

The cool hours exhibit a constant 24-h frequency distribution for the months of May, June and September. For July and August, the distribution reaches a minimum during the mid-day hours. The number of occurrences during the month of May clearly exceeds the corresponding values from

Table 1. Sensation scale for dry cooling power [8]

Cooling power (mcal/cm^2 s^1)	Sensation
< 5	Hot (HO)
5–10	Mild (MI)
11–15	Cool (CL)
16–22	Cold (CD)
23–30	Very cold (VC)
> 30	Extreme cold (EC)

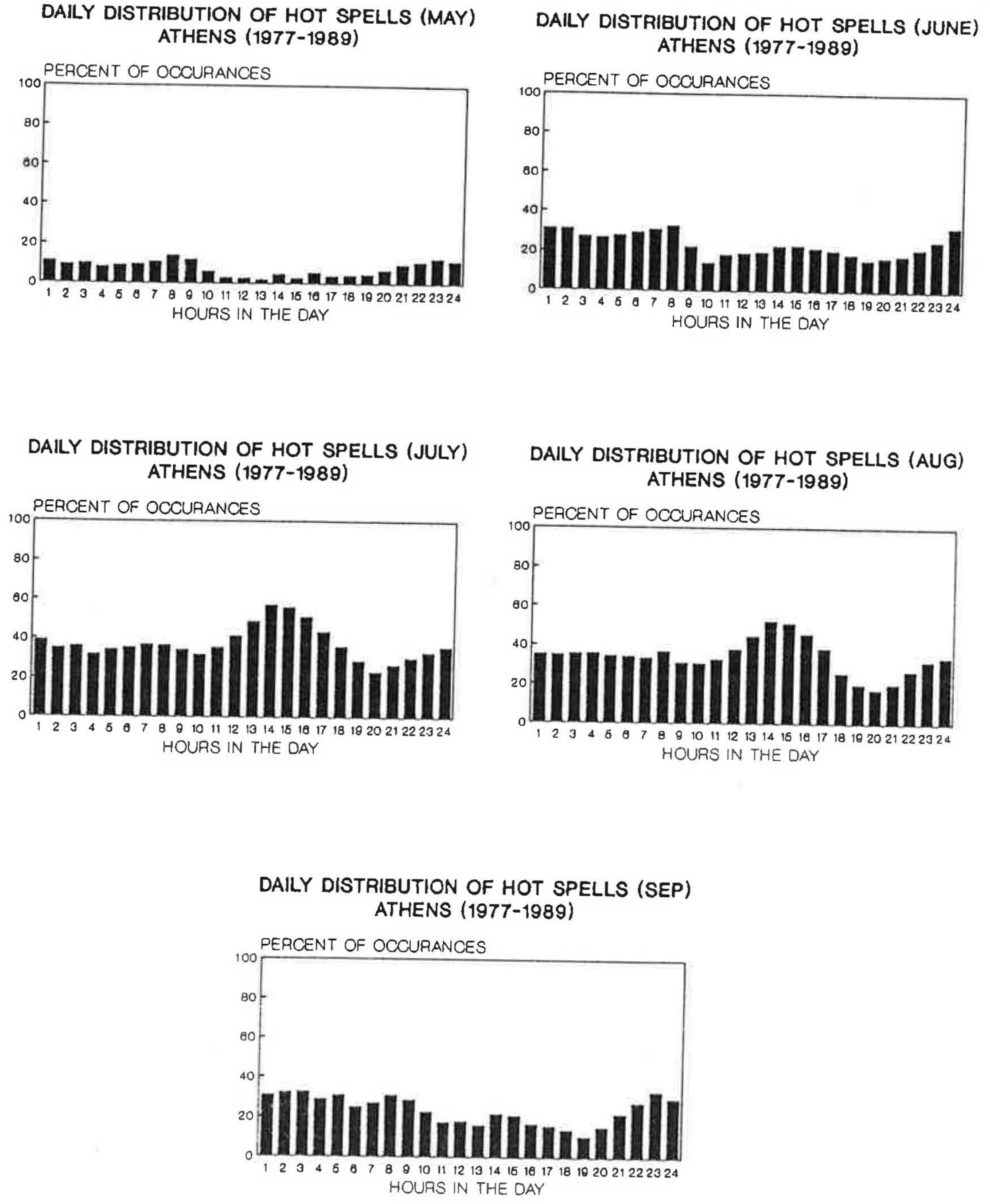

Fig. 1. Daily distribution of hot spells for the cooling season in Athens, Greece (1977–1989).

all other months. This is primarily due to the fact that May cannot be considered as a characteristic summer month, as is the case of September. As a matter of fact, there are a significant number of cool hours in May, more than any of the other months in the cooling season.

The distribution of the hours which correspond to the cold sensation is approximately constant during the whole 24-h period of May and June, with frequencies which do not exceed 28%. In September, the corresponding values do not exceed 11%. In July and August, cold conditions appear only during the night-time hours, with very small absolute values, less than 8%.

The very cold conditions occur only during the months of May and September, with percentages not exceeding 5%. Consequently, their analysis is of no interest, and they should be considered as extreme cases. Similarly, the extra cold conditions do not exhibit any practical interest either, except in the case of September, which are analysed and discussed in a following section.

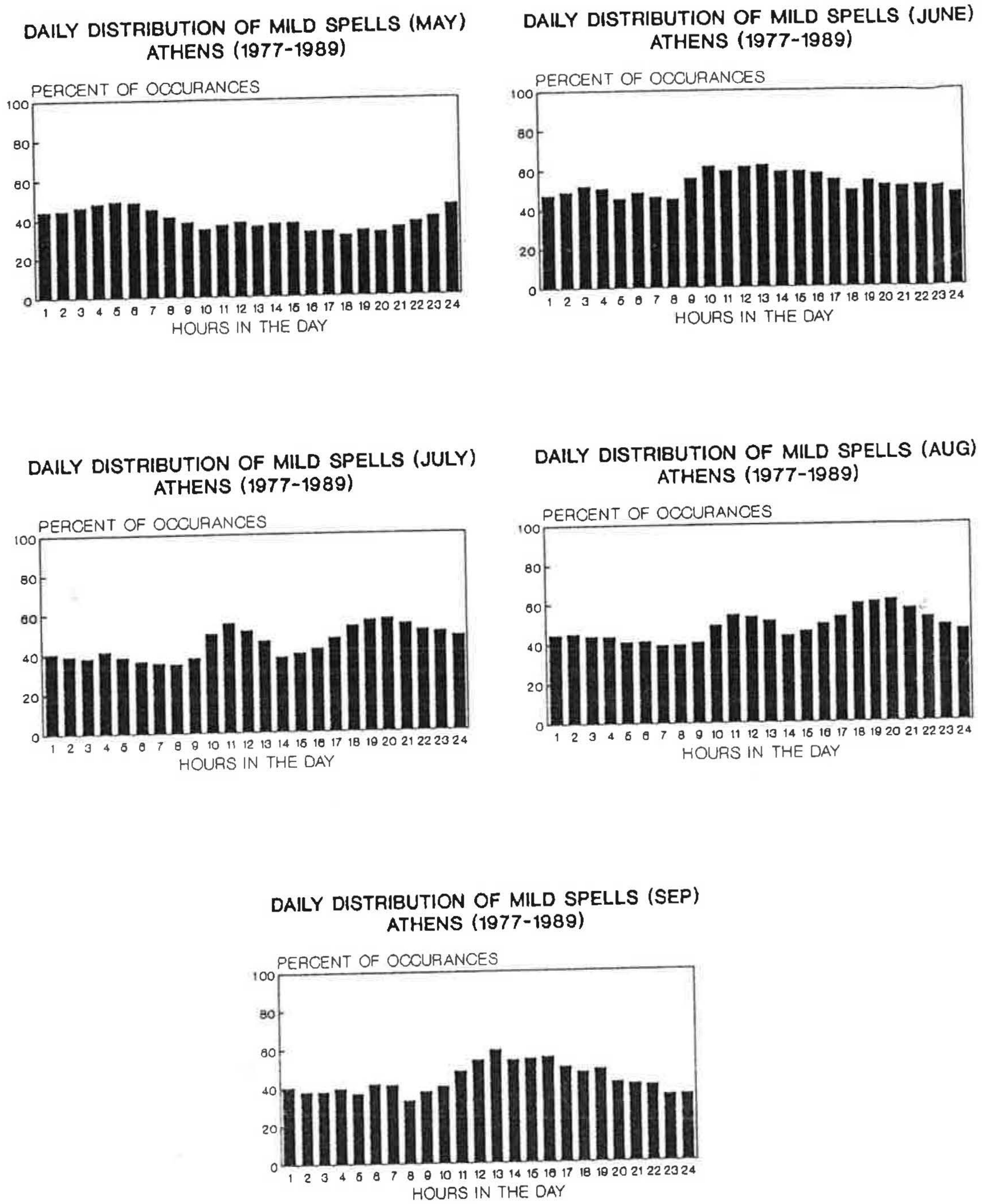

Fig. 2. Daily distribution of mild spells for the cooling season in Athens, Greece (1977–1989).

Analysis of persistence

From the daily distribution of the six different sensations for which we are performing the hourly analysis, it appears that, for most cases, there is a continuous number of successive hours with the same sensation. This observation initiated the following anlaysis for the persistence of a particular sensation in a given time period. An approximation to the persistence of each case of the investigated conditions was based on the number of consecutive hours for a particular sensation, as well as the characteristic behaviour and the persistence of the various sensations under investigation among the different months.

For this purpose, the Besson's coefficient of persistence is used, which is given by the relation:

$$R_b = [(1-P)/(1-P_{i/i})]^{-1} \qquad (2)$$

Table 2. Besson's coefficients of persistence, R_b

Sensation	May	June	July	August	September
Hot	0.504	1.774	2.086	1.851	1.469
Mild	0.939	0.988	1.118	0.988	1.024
Cool	0.683	1.132	1.425	1.344	1.046
Cold	1.132	1.454	1.294	1.492	1.863
V. cold	1.397	1.433	0.000	0.000	2.807
Ex. cold	0.543	0.000	0.000	0.000	3.970

where P is the probability of an event and $P_{i/i}$ is the probability that this event will occur following an occurrence of the same event, which can be calculated by:

$$P_{i/i} = 1 - (S/M) \qquad (3)$$

where

S = total number of spells for a given event
M = total number of hours with an occurrence.

The Besson's coefficient of persistence is equal to zero when there is no persistence ($P_{i/i} = P$) and infinity when the occurrence of an event is always followed by another occurrence of the same event.

The 95% confidence limits of the ratio $1 + R_b$, equation (2), are given by $q/[q \pm 1.96\{pq/N\}^{1/2}]$, provided that R_b is normally distributed. Consequently, an observed value of R_b above the upper confidence limit rejects and null-hypothesis of no persistence. This upper confidence limit is about 1.02 for all cases examined.

The values of R_b are given in Table 2 for every month of the time interval May–September and for every one of the different cases under investigation. As it can be seen, for all months and for the hot, mild, cool, and cold cases, the observed persistence is statistically important. For the case of very cold conditions, there is no persistence during the months of July and August, while in the case of extremely cold conditions, the occurrence of persistence is limited only in May and September.

The persistence of hot, mild, and cool conditions is greater during the month of July, in comparison with the other months, while the persistence of hot hours during the months of June, July and August exceeds all the other cases.

The very high numbers of the R_b coefficient for the cases of very cold and extremely cold conditions, which were observed during September, were due to unusual conditions created by a major weather system over Greece. This resulted in a continuous series of 25 h for the very cold case and a series of 39 consecutive hours for the extremely cold case.

Conditional probabilities. The Eriksson model of persistence

The persistence can also be checked with the calculation of the conditional probability. For example, an hour (n) would be characterized by a particular sensation (i) (HO, MI, CL, CD, VC, or EC) when the condition at the zero hour is available. This is known as the Eriksson model [9].

The Eriksson model can be utilized using the following parameters. Let (P_n) be the probability for the condition (i) on an (n) hour, if the same condition (i) holds on the zero hour, and let (p_n) be the probability for the case (i) on the (n) hour, if the condition (i) does not hold on the zero hour. Let (Q_n) be the probability that the condition (i) does not hold on the (n) hour if it does not hold on the zero hour, and finally let (q_n) be the probability that the condition (i) does not hold on the (n) hour if it holds on the zero hour. The following repetitive correlations can describe all these cases as,

$$P_n = P_{n-1}P_{i|i} + (1 - P_{n-1})P_{i|n0,i} \qquad (4)$$

where $P_1 = P_{i|i}$ and $P_1 = P_{i|n0,i}$, with $\lim_{n\to\infty} P_n = \lim_{n\to\infty} p_n = P$

$$Q_n = Q_{n-1}P_{n0,i|n0,i} + (1 - Q_{n-1})P_{n0,i|i} \qquad (5)$$

$$q_n = q_{n-1}P_{n0,i|n0,i} + (1 - q_{n-1})P_{n0,i|i} \qquad (6)$$

Table 3. The probabilities Q_n, q_n, P_n, p_n together with the general probabilities p and q for hot conditions

		1	2	3	4	5	6	7	8	9	10	11	12
May	Q_n	0.948	0.931	0.925	0.923	0.922	0.922						
	q_n	0.613	0.819	0.887	0.910	0.918	0.921						
	P_n	0.387	0.181	0.113	0.090	0.082	0.079						
	p_n	0.052	0.069	0.075	0.077	0.078	0.078						
	$p = 0.078$, $q = 0.922$												
June	Q_n	0.915	0.860	0.825	0.803	0.789	0.780	0.774	0.770	0.768	0.766	0.765	0.764
	q_n	0.275	0.451	0.564	0.636	0.682	0.711	0.730	0.742	0.750	0.755	0.758	0.760
	P_n	0.725	0.549	0.437	0.364	0.318	0.289	0.270	0.258	0.250	0.245	0.242	0.240
	p_n	0.085	0.140	0.175	0.197	0.211	0.220	0.226	0.230	0.232	0.234	0.235	0.236
	$p = 0.237$, $q = 0.763$												
July	Q_n	0.879	0.796	0.741	0.703	0.678	0.661	0.649	0.642	0.636	0.633	0.630	0.629
	q_n	0.203	0.340	0.432	0.495	0.537	0.566	0.585	0.598	0.607	0.613	0.617	0.620
	P_n	0.797	0.660	0.568	0.505	0.463	0.434	0.415	0.402	0.393	0.387	0.383	0.380
	p_n	0.122	0.204	0.259	0.297	0.322	0.339	0.351	0.358	0.364	0.367	0.370	0.371
	$p = 0.375$, $q = 0.625$												
August	Q_n	0.880	0.802	0.751	0.718	0.697	0.683	0.674	0.668	0.665	0.662	0.660	0.659
	q_n	0.230	0.380	0.477	0.540	0.581	0.608	0.625	0.636	0.643	0.648	0.651	0.653
	P_n	0.770	0.620	0.523	0.460	0.419	0.392	0.375	0.364	0.357	0.352	0.349	0.347
	p_n	0.120	0.198	0.249	0.282	0.303	0.317	0.326	0.332	0.336	0.338	0.340	0.341
	$p = 0.343$, $q = 0.658$												
September	Q_n	0.906	0.850	0.817	0.797	0.785	0.778	0.774	0.772	0.771	0.770		
	q_n	0.312	0.497	0.607	0.673	0.712	0.735	0.749	0.757	0.762	0.765		
	P_n	0.688	0.503	0.393	0.327	0.288	0.265	0.251	0.243	0.238	0.235		
	p_n	0.094	0.150	0.183	0.203	0.215	0.222	0.226	0.228	0.229	0.230		
	$p = 0.231$, $q = 0.769$												

where

$$Q_1 = P_{n0,i|n0,i},\ q_1 = P_{n0,i|i} \text{ with } \lim_{n\to\infty} Q_n = \lim_{n\to\infty} q_n = q,$$

and

$$P_{n0,i|i} = 1 - P_{i|i}, \quad P_{i|n0,1} = 1 - P_{n0,i|i}.$$

The calculated probability values for hot and mild conditions are shown in Tables 3–4. As it can be seen, these values approach the general probabilities p and q relatively quickly, which means that, according to the Eriksson model, one has a correct picture of the observed conditions. The differences between the limit values of Q_n, q_n, P_n and p_n and the estimated values of p and q do not exceed 1–2%, except for the EC case in September, where the difference is of the order of 13%. This high percentage must be attributed to the extremely large number of consecutive EC hours (39) which are included in the time series.

For the hot conditions, after 6 h in May, 12 h for July and August, and 10 h for September, the phenomenon of persistence stops. This occurs when the differences between P_n and p_n, and between Q_n and q_n, reach a minimum value. For the mild conditions, the persistence stops after 8 h in May and after 9 h for the remaining months.

For the cool conditions, the persistence stops after 7 h in May and June, and after 8 h for the remaining months. For the cold conditions, the persistence stops after 8 h for all the months except for July. For this particular month, it stops after 7 h, since July is the hottest month of the year and the local Etesian winds have not yet reached the stage of their highest frequency. The very cold conditions exhibit a persistence of 8 h during May, June and September, while there is no meaningful persistence of similar conditions during July and August. Finally, for the extremely cold conditions, it is not possible to define a meaningful persistence period for any of these months, not even for September, for which, as we have already mentioned, there is a great difference between conditional and unconditional probabilities.

Finally, the persistence of the hot conditions according to Table 3 appears to be in agreement with the values of the persistence coefficient R_b (see Table 2). There is a tendency for higher values during the summer months (June–August) in comparison with May, and a less obvious one in comparison with September.

Table 4. The probabilities Q_n, q_n, P_n, p_n together with the general probabilities p and q for mild conditions

		1	2	3	4	5	6	7	8	9	10	11	12
May	Q_n	0.798	0.700	0.653	0.630	0.619	0.614	0.611	0.609				
	q_n	0.314	0.466	0.540	0.575	0.592	0.600	0.605	0.606				
	P_n	0.686	0.534	0.460	0.425	0.408	0.400	0.396	0.394				
	p_n	0.202	0.300	0.347	0.370	0.381	0.386	0.389	0.391				
	$p = 0.391$, $q = 0.609$												
June	Q_n	0.749	0.625	0.563	0.532	0.517	0.509	0.505	0.503	0.502	0.502		
	q_n	0.253	0.378	0.440	0.471	0.486	0.494	0.495	0.498	0.500	0.501		
	P_n	0.747	0.622	0.560	0.529	0.514	0.506	0.505	0.502	0.500	0.499		
	p_n	0.251	0.375	0.437	0.468	0.483	0.491	0.495	0.497	0.498	0.498		
	$p = 0.498$, $q = 0.502$												
July	Q_n	0.788	0.676	0.617	0.586	0.569	0.560	0.555	0.553	0.552			
	q_n	0.260	0.397	0.470	0.508	0.528	0.539	0.545	0.548	0.549			
	P_n	0.740	0.603	0.530	0.492	0.472	0.461	0.455	0.452	0.451			
	p_n	0.212	0.324	0.383	0.414	0.431	0.440	0.445	0.447	0.448			
	$p = 0.450$, $q = 0.550$												
August	Q_n	0.756	0.635	0.575	0.545	0.530	0.522	0.518	0.516	0.515			
	q_n	0.259	0.388	0.452	0.483	0.500	0.508	0.512	0.514	0.515			
	P_n	0.741	0.612	0.548	0.516	0.500	0.492	0.488	0.486	0.485			
	p_n	0.244	0.365	0.425	0.455	0.470	0.478	0.482	0.484	0.485			
	$p = 0.485$, $q = 0.515$												
September	Q_n	0.765	0.646	0.586	0.556	0.541	0.533	0.529	0.527	0.526			
	q_n	0.260	0.391	0.457	0.491	0.508	0.517	0.521	0.523	0.524			
	P_n	0.740	0.609	0.543	0.509	0.492	0.483	0.479	0.477	0.476			
	p_n	0.235	0.354	0.414	0.444	0.459	0.467	0.471	0.473	0.474			
	$p = 0.474$, $q = 0.526$												

The corresponding starting and ending dates of the longest series of the hot hours for every month, are summarized in Table 5. Cross-referencing this information with the *European Meteorological Bulletin* [10], shows that, for all periods, there was no particular synoptic weather system over Greece. As a result, the prevailing high temperatures and low wind speed near the ground surface assisted the persistence of hot conditions for a high number of consecutive hours.

On the other hand, there was a strong cold anti-cyclone (with a 1035 mbar barometric pressure at its centre) which was extended from north of Greece over the Balkan peninsula during the period of the extra cold conditions, 39 consecutive hours 01:00 LST of 28-9-1977 to 15:00 LST of 29-9-1977. This system influenced the weather in Greece, giving a NNE major current with a mean daily wind speed of about 12.7 and 11.0 m/s, respectively. This shifted cold air masses over Greece with minimum temperatures at 14.0 and 12.2°C, respectively.

CONCLUDING REMARKS

Based on the 13-yr analysis, the appearance of hot and mild conditions during a 24-h period are significant during the months of June/July/August and May/September, respectively, while the other cases do not exhibit any statistical significance.

Table 5. Monthly maximum consecutive hours of hot periods for Athens (1977–1989)

Month	Consecutive hours	Starting		Ending	
		Hour	Date	Hour	Date
May	14	0900	1/5/1983	1000	2/5/1983
June	109	0800	24/6/1983	2000	28/6/1983
July	96	0800	8/7/1980	1900	12/7/1980
August	46	0700	13/8/1977	0400	15/8/1977
September	45	2200	6/9/1984	1800	8/9/1977

According to Table 3, the probabilities from the Eriksson model for the hot conditions exhibit the highest persistence for 10–12 continuous hours in July and August and similar values, around 0.2, in June and September, while they are significantly lower in May. Further theoretical analysis of the persistence of the various conditions should be limited to the hot and mild conditions. In any event, these conditions are of particular interest since they are directly related with the sensation of discomfort during the summer months.

REFERENCES

1. M. Santamouris, Natural cooling techniques. In *Proc. Conference Passive Cooling* (Edited by E. Aranovich, T. Steemers and E. Oliveira Fernandes), E.E.C., D.G. 12, Ispra (1990).
2. Predicasts Inc., *Predicasts Forecasts*, Issue 108, 4th Quarter, Refrigeration and Air Conditioning Equipment Data (1987).
3. M. Antinucci, B. Fleury, J. Lopez d'Asiain, E. Maldonado, M. Santamouris, A. Tombazis and S. Yannas, *Horizontal Study on Passive Cooling* (Edited by M. Santamouris). Building 2000 Research Project, EEC, D.G. 12 (1990).
4. I. Tselepidaki and M. Santamouris, *Energy Bldgs.* **17**, 243 (1991).
5. I. Tselepidaki, M. Santamouris and D. Melitsiotis, Analysis of the summer ambient temperature for cooling purposes. Submitted to *Sol. Energy*. In press (1992).
6. B. D. Giles, C. Balafoutis and P. Maheras, *Int. J. Biometeorol.* **34**, 98 (1990).
7. T. D. Potter and L. E. Olsson, Climate and tourist health. An overview of the World Meteorological Organization activities. *Proc. 2nd Int. Conf. on Tourism Health*, Rimini, Italy (1989).
8. H. E. Landsberg, *The Assessment of Human Bioclimate*. Technical Report No. 123, Secretariat of the World Meteorological Organization, Geneva, Switzerland (1972).
9. B. Eriksson, *Tellus* **XVII**, 484 (1965).
10. *European Meteorological Bulletin*, Amtsblatt des Deutschen Wetterdienstes, Druck und Verlag: Deutscher Wetterdienst-Zentralamt.

Energy Convers. Mgmt Vol. 34, No. 2, pp. 147–152, 1993
Printed in Great Britain.

0196-8904/93 $5.00 + 0.00

TECHNICAL NOTE

THERMAL EFFICIENCY OF COLLECTION-CUM-STORAGE SOLAR WATER HEATER

G. N. TIWARI and A. K. SINGH

Centre for Energy Studies, Indian Institute of Technology, Hauz Khas, New Delhi-110 016, India

(Received 5 August 1991; received for publication 17 April 1992)

Abstract—In this Technical Note, an analytical expression for the thermal efficiency of a collection-cum-storage water heater, in terms of design and climatical parameters, has been derived. The effects of the design and climatical parameters on the efficiency have been discussed analytically which are in accordance with the results obtained by earlier workers. A good agreement between experimental and theoretical results was obtained.

Solar energy   Water heater   Thermal efficiency

NOMENCLATURE

C_w = Specific heat of water (J/kg °C)
h_0 = Heat transfer coefficient per unit length (W/m °C)
h_1 = Heat transfer coefficient between absorber and ambient through glass cover (W/m^2 °C)
h_2 = Heat transfer coefficient between absorber and water (W/m^2 °C)
h_b = Heat transfer coefficient between absorber and ambient through insulation (W/m^2 °C)
h_i = Heat transfer coefficient from bottom insulation to ambient (W/m^2 °C)
$I(t)$ = Solar intensity (W/m^2)
K_i = Thermal conductivity of insulation (W/m^2 °C)
L_i = Thickness of insulation (m)
L = Length of heat exchanger (m)
m_w = Mass flow rate (kg/m^2 s)
M_w = Mass of water heater (kg/m^2)
Q_w = Thermal energy transfer to heat exchanger (W/m^2)
Q = Energy available at blackened surface (W/m^2)
t = Time coordinate (s)
T_a = Instantaneous ambient air temperature (°C)
T_b = Instantaneous temperature of absorber (°C)
T_w = Instantaneous temperature of water (°C)
T_{wi} = Initial temperature of water at $t = 0$ (°C)
n = Efficiency of system
$(\alpha\tau)$ = Product of absorptivity of blackened surface and transmittivity of glass cover

INTRODUCTION

The solar water heater is basically classified as a conventional or collection-cum-storage water heater. In a conventional water heater, there are two units, namely the collector and the insulated storage units. The water is heated in the collector by solar energy and is transferred to insulated tanks under thermosyphon as well as forced circulation modes [1]. When the water is heated and stored in the same unit, the system is called a collection-cum-storage water heater, which is one of the two types, viz. built-in storage or shallow solar pond water heater. In the built-in storage water heater, the solar energy is absorbed at a blackened surface at the top of the water column [Fig. 1(a)], while solar energy is absorbed at a blackened surface below the water column in the shallow solar pond [Fig. 1(b)]. The works on collection-cum-storage water heaters have been reviewed by Bansal [2] in 1983. Later on, an earlier analysis was extended by incorporating the effects of various parameters, viz. intermittent mass flow rate, optimization of system connected in series, reduction of upward heat loss, etc. by various workers.